Matthijs Oudkerk, MD, PhD
Carl G. Torres, PhD
Bin Song, MD
Matthias König, MD
Jan Grimm, MD
Jaime Fernandez-Cuadrado, MD
Bart Op de Beeck, MD
Moritz Marquardt, MS
Pieter van Dijk, MS
Jan Cees de Groot, MD, PhD

Index terms:
Computed tomography (CT), comparative studies, 761.12115
Contrast media
Liver neoplasms, diagnosis, 761.312, 761.3192, 761.3194, 761.3198, 761.32, 761.323, 761.33
Magnetic resonance (MR), comparative studies, 761.12143

Published online before print
10.1148/radiol.2232010318
Radiology 2002; 223:517–524

Abbreviations:
HCC = hepatocellular carcinoma
Mn-DPDP = mangafodipir trisodium
ROC = receiver operating characteristic

[1] From the Dept of Radiology, Daniel den Hoed Cancer Ctr, Univ Hosp Rotterdam, the Netherlands (M.O., B.S., P.v.D.); State Univ and Academic Hosp of Groningen, Hanzeplein 1, PO Box 30.001, 9700 RB Groningen, the Netherlands (M.O., J.C.d.G.); First Univ Hosp, West China Univ of Med Sciences, Chengdu, People's Republic of China (B.S.); Nycomed Amersham, Oslo, Norway (C.G.T.), and Munich, Germany (M.M.); Ruhr Univ Clinic, Bochum, Germany (M.K.); Christian-Albrechts Univ, Kiel, Germany (J.G.); Hosp La Paz, Madrid, Spain (J.F.C.); and Univ Hospital, Free Univ Brussels, Belgium (B.O.d.B.). From the 1999 RSNA scientific assembly. Received Jan 16, 2001; revision requested Mar 5; final revision received Oct 4; accepted Oct 15. **Address correspondence to** M.O. (e-mail: *m.oudkerk@rad.azg.nl*).

Author contributions:
Guarantors of integrity of entire study, M.O., C.G.T., P.v.D.; study concepts and design, M.O., C.G.T., P.v.D.; literature research, B.S., C.G.T., P.v.D.; clinical studies, M.K., J.G., J.F.C., B.O.d.B.; data acquisition, P.v.D., M.K., J.G., J.F.C., B.O.d.B.; data analysis/interpretation, C.G.T., P.v.D., J.C.d.G., M.O.; statistical analysis, M.M.; manuscript preparation, B.S., C.G.T., P.v.D., J.C.d.G.; manuscript definition of intellectual content, M.O., C.G.T., P.v.D.; manuscript editing, B.S., C.G.T., P.v.D., J.C.d.G., M.O.; manuscript revision/review, M.O., B.S., C.G.T., P.v.D., M.K., J.G., J.F.C., B.O.d.B., J.C.d.G.; manuscript final version approval, M.O., P.v.D., C.G.T.

Characterization of Liver Lesions with Mangafodipir Trisodium–enhanced MR Imaging: Multicenter Study Comparing MR and Dual-Phase Spiral CT[1]

PURPOSE: To evaluate whether mangafodipir trisodium (Mn-DPDP)–enhanced magnetic resonance (MR) imaging surpasses dual-phase spiral computed tomography (CT) in differentiating focal liver lesions.

MATERIALS AND METHODS: One hundred forty-five patients who had or were suspected of having focal liver lesions were included in a multicenter study and underwent dual-phase spiral CT and enhanced MR imaging. Image interpretations performed by independent experienced radiologists were compared with the final diagnosis that was based on all available clinical information (including histopathologic findings in 77 patients) and that was determined with consensus. Differences in classifications by using either enhanced MR imaging or dual-phase spiral CT were analyzed with the McNemar test, and receiver operating characteristic (ROC) curves were used to compare the diagnostic performance of enhanced MR imaging and dual-phase spiral CT.

RESULTS: Lesion classification was correct in 108 (74%) patients with enhanced MR imaging and in 83 (57%) with dual-phase spiral CT ($P = .001$). Lesions were correctly classified as either malignant or benign in 123 (85%) patients with enhanced MR imaging and in 98 (68%) with dual-phase spiral CT ($P = .001$). Classification of lesions as either hepatocellular or nonhepatocellular was correct in 130 (90%) patients with enhanced MR imaging and in 93 (64%) with dual-phase spiral CT ($P = .001$). These differences remained when analyses were restricted to histopathologically confirmed diagnoses. Comparison of the ROC curves illustrated that enhanced MR imaging performance surpassed that of dual-phase spiral CT.

CONCLUSION: Mn-DPDP–enhanced MR imaging is superior to dual-phase spiral CT in classification of focal liver lesions.

In planning the therapeutic approach for patients who have or are suspected of having liver lesions, imaging is one of the major sources of information (1). Although ultrasonography (US) will depict most of the focal liver lesions, characterization of the nature of such lesions often depends on an additional imaging evaluation, sometimes followed by a histopathologic examination. The two principal modalities for the additional imaging evaluation of the liver, computed tomography (CT) and magnetic resonance (MR) imaging, have undergone marked technical advances over the past few years (1,2). As to focal liver lesion detection, it is now generally accepted that contrast material–enhanced CT scanning (dynamic or multiphasic) is roughly comparable to unenhanced MR imaging with optimized pulse sequences for liver imaging (3,4) and inferior to contrast-enhanced MR imaging with gadolinium chelates (5–7), iron oxide compounds (8–10), and manganese

chelates (11–14). Lesion characterization, on the other hand, has not been as intensively compared as lesion detection. Results of studies comparing lesion characteristics by using these two modalities are inconclusive, mainly owing to difficulty to maintain the comparability of these two modalities in the study design. For convincing comparisons, both modalities need to represent state-of-the-art techniques, which implies that liver-specific rather than nonspecific contrast agents should be used when available. Mangafodipir trisodium (Mn-DPDP) has a special affinity for hepatocytes and thus represents such a liver-specific MR contrast agent (12,13,15). Following intravenous administration, the Mn-DPDP chelate dissociates slowly, and the manganese is taken up by the hepatocytes. This leads to an increase in signal intensity of normal liver parenchyma on the T1-weighted image caused by T1 shortening and, thereby, to an increase in contrast between normal and abnormal tissue (13,16). Because there are no liver-specific CT contrast agents available, it would seem that Mn-DPDP–enhanced MR imaging might allow a more specific diagnosis to be established for focal liver lesions than dual-phase spiral CT.

The purpose of this prospective multicenter clinical phase 3 study was to compare the ability to differentiate focal liver lesions by using Mn-DPDP–enhanced MR imaging and contrast-enhanced dual-phase spiral CT, both of which represent state-of-the-art techniques (11,13,16–23).

MATERIALS AND METHODS

Study Population

Eligible patients were to be conscious, cooperative, and scheduled to be radiologically examined because they had or were suspected of having liver lesions (as seen at a US, CT, or MR examination within 4 weeks prior to inclusion) so that different types of benign and malignant focal liver lesions could be distinguished. Medical history, possible risk factors, and concomitant medication were noted prior to Mn-DPDP–enhanced MR imaging or dual-phase spiral CT.

Patients were excluded if they were less than 18 years old; they were pregnant or breast-feeding; they had a clinically unstable condition or an active, serious, and/or life-threatening disease (eg, life expectancy less than a month); they had severe unrelieved obstructive hepatobiliary disease (serum bilirubin, >47.5 μmol/L [>2.5 mg/100 mL]); they had severe renal impairment (serum creatinine, >133 μmol/L [>1.5 mg/100 mL]); they had or were suspected of having pheochromocytoma; they had contraindications for MR imaging or CT; they had received or were scheduled to receive another contrast medium (for MR imaging, radiography, or US) within 12 hours prior to or 24 hours after the proposed dual-phase spiral CT and Mn-DPDP–enhanced MR examinations; they were previously included in this trial or they were simultaneously or had previously participated in or planned to participate in another clinical trial with intake of an investigational drug within the 7 days prior to or after participation in this trial.

From December 1996 to September 1998, 152 consecutive patients (62 [41%] women, 90 [59%] men; mean age, 59 years; age range, 28–83 years) were enrolled in the present six-center (Netherlands, Belgium, Spain, Germany [including two centers] and England) open-label study. Written informed consent was obtained from each patient after the nature of the procedures had been fully explained. Approval from the ethics committee of each center was also obtained. After dual-phase spiral CT, Mn-DPDP–enhanced MR imaging was performed minimally 24 hours later and maximally a week later.

Imaging Methods

In all participants, transverse dual-phase spiral CT scans and Mn-DPDP–enhanced MR images were obtained and included the whole liver during one breath hold (after maximal inspiration) in cranial caudal direction.

For dual-phase spiral CT (Somatom Plus 4; Siemens, Erlangen, Germany), after an initial scout scan, images (120 kV; 210 mA; section thickness, 5 mm; table speed, 10 mm/sec; rotation, 1/sec; acquisition time, approximately 20 seconds; field of view, 350 mm) were acquired before administration of contrast material. Afterward a total of 150 mL (administered at 4 mL/sec for 37.5 seconds) of iohexol (Omnipaque 300; Nycomed Imaging, Oslo, Norway) was administered intravenously with a programmed CT injector (EnVision; Medrad, Indianola, Pa), and scans were obtained 21 and 66 seconds after the start of the injection during the arterial and portal phases, respectively.

For Mn-DPDP–enhanced MR imaging, a 1.5-T unit (Magnetom Vision; Siemens, Erlangen, Germany) was used. After initial scout images, precontrast images with a section thickness of 5 mm (no gap) and T1-weighted gradient-echo (repetition time msec/echo time msec, 170/4.4; flip angle, 80°; field of view, 350 mm; number of sections, 21) and T2-weighted turbo spin-echo MR images (3,200/138; flip angle, 180°; field of view, 350 mm; number of sections, 10) were obtained with a circular-phased body phased-array coil (total imaging time, approximately 1 hour). Hereafter, 0.005 mmol (0.5 mL) per kilogram of body weight of Mn-DPDP (Teslascan; Nycomed Imaging, Oslo, Norway) was administered intravenously (slow injection at 2.5 mL/min). Mn-DPDP–enhanced MR imaging was initiated 15–30 minutes after administration of the contrast agent with the same protocol and sequences as described previously. Adverse events were recorded for both imaging modalities.

Image Interpretation

All Mn-DPDP–enhanced MR images and dual-phase spiral CT scans were centrally collected, and hard copies were interpreted off site by experienced radiologists who were blinded to any clinical, laboratory, or other imaging information and who were chosen from nonparticipating medical institutions. Independent from each other, an MR radiologist (J.F.C.) evaluated the Mn-DPDP–enhanced MR images, whereas a CT radiologist evaluated the dual-phase spiral CT scans. In case their diagnoses were different, the images were reinterpreted by two other radiologists without knowledge of the prior interpretation. In case of disagreement between the first interpretation (determined by the MR and CT radiologists) and the second interpretation (determined by two other radiologists) of the same image, a consensus panel, including the two original radiologists (CT and MR radiologists) plus an independent third, decided on the final interpretation.

For those cases in which the CT and MR radiologists agreed, the final interpretation was the first interpretation that they determined. Each reader was required to answer several questions for each patient regarding the lesion (absent vs present), the nature of the lesion (malignant vs benign), the type of the lesion (hepatocellular vs nonhepatocellular), and the most likely etiologic diagnosis. Lesions were characterized according to their characteristic imaging appearance on the Mn-DPDP–enhanced MR image or dual-phase spiral CT scan. On Mn-DPDP–enhanced MR images, lesions were considered of hepatocytic origin if there was enhancement on T1-weighted Mn-DPDP–enhanced MR images. Further

TABLE 1
Diagnostic CT and MR Imaging Criteria for Classification of Focal Liver Lesions

Imaging Feature	Dual-Phase Spiral CT			Mn-DPDP-enhanced MR Imaging		
	Type of Image	Rim Appearance	Lesion Appearance	Type of Image	Rim Appearance	Lesion Appearance
Benign, hepatocellular Adenoma						
	Plain image	Low attenuation	Isoattenuation to high attenuation	Plain T1-weighted	Hypointensity	Isointensity to hyperintensity
	Arterial phase	No enhancement	Strong enhancement	Plain T2-weighted	Mild hyperintensity	Mild hyperintensity
	Portal phase	Enhancement	Slow washout	Mn-DPDP–enhanced T1-weighted	Late enhancement	Nonhomogeneous enhancement
Focal nodular hyperplasia						
	Plain image	No rim	Isoattenuation	Plain T1-weighted	No rim	Isointensity
	Arterial phase	No rim	Strong, homogeneous enhancement	Plain T2-weighted	No rim	Isointensity, with hyperintense central scar
	Portal phase	No rim	Quick washout	Mn-DPDP–enhanced T1-weighted	No rim	Strong, homogeneous enhancement with delayed scar enhancement
Benign, nonhepatocellular, hemangioma						
	Plain image	No rim	Low attenuation	Plain T1-weighted	No rim	Hypointensity
	Arterial phase	No rim	Nodular and peripheral enhancement	Plain T2-weighted	No rim	Marked hyperintensity
	Portal phase	No rim	Filling, slightly high attenuation	Mn-DPDP–enhanced T1-weighted	No rim	Peripheral nodular late enhancement
Malignant, hepatocellular, hepatocellular carcinoma						
	Plain image	Low attenuation	Isoattenuation, mosaic enhancement	Plain T1-weighted	Hypointensity	Isointensity to hyperintensity, mosaic enhancement
	Arterial phase	Minimal enhancement	Strong, heterogeneous enhancement	Plain T2-weighted	Hyperintensity	Hypointensity and hyperintensity
	Portal phase	Isoattenuation to high attenuation	Slow washout	Mn-DPDP–enhanced T1-weighted	Delayed enhancement	Nonhomogeneous early enhancement
Malignant, nonhepatocellular, metastasis						
	Plain image	No rim	Low attenuation	Plain T1-weighted	No rim	Hypointensity
	Arterial phase	No rim	Minimal enhancement	Plain T2-weighted	No rim	Minimal enhancement, peripheral edema
	Portal phase	No rim	Peripheral ring enhancement, slow washout	Mn-DPDP–enhanced T1-weighted	No rim	Peripheral ring enhancement with hypointense center

classification was possible with examination of the enhancement pattern of the lesion. For the most common focal liver lesions, the discriminating imaging characteristics on MR images and dual-phase spiral CT scans are listed in Table 1.

Regarding the nature of the lesion, the readers were additionally asked to rate their confidence level for diagnosing the presence of a malignant lesion on a five-point scale (definitely not, probably not, possibly, probably, definitely). The confidence level of the reader on the imaging diagnosis was also rated on a five-point scale. When patients had more than one type of liver lesion, the clinically most important lesion was marked by the on-site radiologists for evaluation by the independent off-site readers to ensure that identical lesions were evaluated by using both imaging modalities.

Forming the Reference Diagnosis

The off-site interpretation of dual-phase spiral CT scans and Mn-DPDP–enhanced MR images was compared with the reference diagnosis, which was formed on site by means of interpretation of all available data in each patient. These data included all imaging data (findings of US, CT, MR imaging, and other imaging if available), clinical data, laboratory data, as well as data from follow-up examinations. Follow-up duration was a minimum of 3 months and a maximum of 1 year. Follow-up examinations were part of the clinical routine and not part of the study protocol. We attempted to obtain histopathologic confirmation for reference diagnoses if lesions were not considered benign or if they were not apparent metastases from a known primary tumor.

Statistical Analyses

Differences in baseline characteristics between patients with and those without histopathologic information were analyzed by using *t* tests for continuously distributed variables and χ^2 tests for all other variables. For each imaging modality, accuracy, sensitivity, and specificity of each scored item were calculated by using the reference diagnosis as the reference standard. The differences between Mn-DPDP–enhanced MR imaging and dual-phase spiral CT with regard to these measures were analyzed by using the McNemar test (two-tailed). We analyzed whether the diagnostic confidence level for malignancy of a lesion was worse than, equal to, or better with Mn-DPDP–

enhanced MR imaging or with dual-phase spiral CT by using the binomial test (two-tailed).

Additionally, performance of Mn-DPDP–enhanced MR imaging and dual-phase spiral CT in indicating malignancy of focal liver lesions was compared and analyzed by using receiver operating characteristic (ROC) curves (one-tailed). For all analyses we used an α of 5%. The ROC analysis was performed with dedicated software (Rockit; Charles E. Metz, University of Chicago, Ill), and all other analyses were performed with standard statistical software (SAS; SAS Institute, Cary, NC). Since overall results with either the consensus off-site readings or the first off-site readings were identical, we included only our findings concerning the first readings.

RESULTS

Complete data were acquired for 145 of 152 eligible patients. One patient withdrew, two had a reference diagnosis of lesions classified as "other," which could not be matched to diagnoses determined with imaging findings, and with four patient technical problems with the CT occurred, such that classification of lesions was impossible. Only one patient experienced an adverse event (thirst) after the Mn-DPDP administration. No other adverse events related to drugs used in the trial occurred. Mean age of the 145 participants was 58.3 years (61 [42%] women, 84 [58%] men]). A disagreement in classification with Mn-DPDP–enhanced MR imaging and dual-phase spiral CT occurred in 43 patients. Although 10 patients were suspected of having focal liver lesions when they were included in the study, no lesions could be detected by using either Mn-DPDP–enhanced MR imaging or dual-phase spiral CT. Histopathologic information was available for deciding on the reference diagnosis in 77 (57%) of 135 detected lesions. For the other 58 (43%) lesions, biopsy was considered unethical because lesions were considered benign lesions or metastases from a known primary tumor.

Sixty-five (84%) of 77 patients with histopathologic information had malignant lesions versus 32 (47%) of 68 patients without such information ($P < .001$). There was no difference in age or sex distribution across these groups. Detected liver lesions were diagnosed as 70 liver metastases, 21 hepatocellular carcinomas (HCCs), 12 hemangiomas, eight cysts, six instances of focal nodular hyperplasia, five adenomas, three regenerative nodules, two scars, two cholangiocarcinomas, one adenocarcinoma, one non-Hodgkin lymphoma, one cancer of the gallbladder, one sarcoma, one calcification, and one abscess. Illustrative cases are shown in Figures 1–4.

Table 2 shows that in the 145 patients, classification was more often correct with Mn-DPDP–enhanced MR imaging than with dual-phase spiral CT ($P = .001$). This difference remained when analyses were confined to the 77 patients with histopathologically confirmed diagnoses ($P = .004$). When analyzing all 145 patients, the classification was correct with Mn-DPDP–enhanced MR imaging but wrong with dual-phase spiral CT in 34 cases, whereas in nine cases the classification was correct with dual-phase spiral CT but wrong with Mn-DPDP–enhanced MR imaging. By confining the analysis to the 77 patients with histopathologically confirmed diagnoses, these data were 19 and five cases, respectively.

Concerning the differentiation between benign or malignant lesions, Mn-DPDP–enhanced MR imaging more often than dual-phase spiral CT evaluation led to the correct diagnosis (Table 2). This was found for the analyses in all 145 patients ($P = .001$) and for those in the 77 patients with histopathologically confirmed diagnoses ($P = .001$). In the analysis of all 145 patients, we found that in 33, diagnosis of a lesion as either malignant or benign was correct with Mn-DPDP–enhanced MR imaging but wrong with dual-phase spiral CT, while the diagnosis was correct with dual-phase spiral CT and wrong with Mn-DPDP–enhanced MR imaging in eight. When the analysis was confined to the patients with histopathologically confirmed diagnosis, these data were 16 and two, respectively.

Sensitivity and specificity for the differentiation between malignant and benign lesions with Mn-DPDP–enhanced MR imaging were better than they were with dual-phase spiral CT (Table 3) and remained better when the analyses were restricted to the patients with histopathologic confirmation. We summarized and compared the diagnostic performance regarding the evaluation of malignancy with both imaging modalities by constructing ROC curves (Fig 5). Because the area under the ROC curve for Mn-DPDP–enhanced MR imaging is larger than the area under the ROC curve for dual-phase spiral CT, the diagnostic performance with Mn-DPDP–enhanced MR imaging for this classification surpasses that of dual-phase spiral CT ($P = .034$).

Table 2 shows that the classification as either hepatocellular or nonhepatocellular was correct more often with Mn-DPDP–enhanced MR imaging than with dual-phase spiral CT. This is true for both the whole-group analyses ($P = .001$) and for the subgroup with histopathologically confirmed diagnoses ($P = .033$). In 46 of 145 cases, diagnosis of a lesion as either hepatocellular or nonhepatocellular was correct with Mn-DPDP–enhanced MR imaging but wrong with dual-phase spiral CT, whereas in nine, the diagnosis was correct with dual-phase spiral CT and wrong with Mn-DPDP–enhanced MR imaging. Confining the analysis to the histopathologically confirmed diagnoses, these data were 16 and six, respectively. In terms of sensitivity and specificity, Mn-DPDP–enhanced MR imaging performed better than dual-phase spiral CT in the whole group as well as in the group with histopathologic confirmation (Table 3).

Incorrect diagnoses with dual-phase spiral CT occurred in a wide disease spectrum ranging from metastasis, HCC, and cholangiocarcinoma to hemangioma and focal nodular hyperplasia. Incorrect diagnoses determined exclusively with Mn-DPDP–enhanced MR imaging were almost all metastases, particularly those originating from primary colorectal carcinoma. In these patients, the Mn-DPDP–enhanced MR images demonstrated some hyperintense ring- or rim-like zones at the periphery of the tumor, with varying degrees of enhancement (Fig 4).

Lesions were correctly classified as malignant by using Mn-DPDP–enhanced MR imaging as well as by using dual-phase spiral CT in 55 of 97 patients. In the 55 lesions, radiologists were more confident diagnosing malignancy with Mn-DPDP–enhanced MR imaging than with dual-phase spiral CT in 34 (62%) patients, equally confident in 17 (31%), and less confident in four (7%). Taking into account all correct diagnoses, interpreters of Mn-DPDP–enhanced MR images were extremely confident of their diagnosis at review of 55 (51%) of 108 MR images versus five (6%) of 83 dual-phase spiral CT images.

DISCUSSION

Results from this multicenter trial, in which state-of-the-art liver imaging techniques for characterizing focal liver lesions were compared, indicate that Mn-

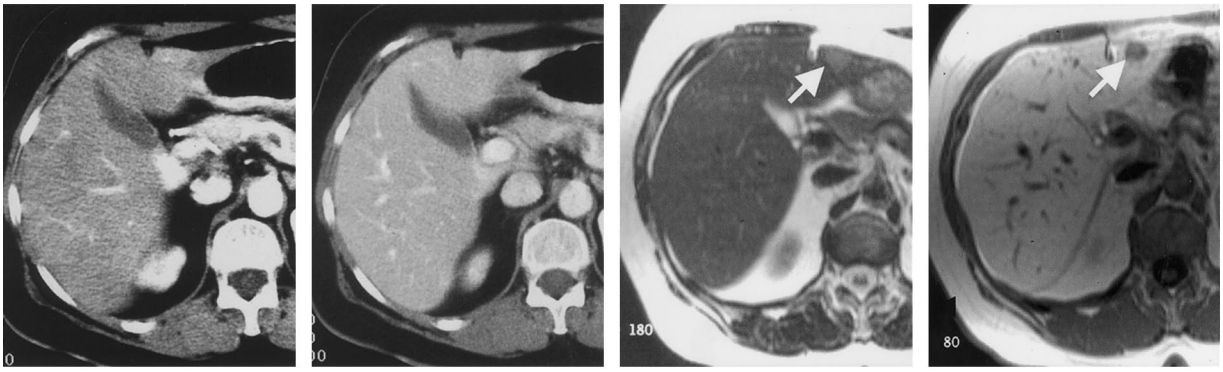

a. b. c. d.

Figure 1. Images show colorectal carcinoma in a 62-year-old woman who was evaluated for staging of the disease. Retrospectively, transverse spiral CT scans obtained in the **(a)** arterial and **(b)** portal phases showed a poorly defined region in the left hepatic lobe, with slight enhancement in the arterial phase, which was not visualized in the portal phase. Readers of the CT scans did not identify the lesion. On the transverse **(c)** Mn-DPDP–enhanced T2-weighted (3,200/138; flip angle, 180°) and **(d)** Mn-DPDP–enhanced T1-weighted (170/4.4; flip angle, 80°) MR images, the lesion was clearly visualized (arrow), and readers of the Mn-DPDP–enhanced MR images classified the lesion as metastatic disease. The final histopathologic diagnosis was liver metastasis from colon carcinoma.

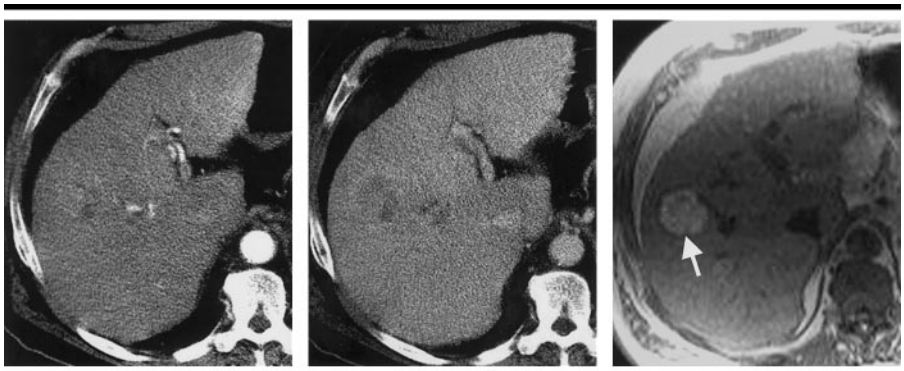

a. b. c.

Figure 2. Transverse images show HCC in a 51-year-old man. Images were arranged to depict the same lesion at the same level in the anterior segment of the right hepatic lobe. Transverse dual-phase spiral CT scans show that the lesion is inhomogeneously enhanced on the image obtained during the **(a)** arterial phase and predominantly hypoattenuating on the image obtained during the **(b)** portal venous phase. Despite these features, readers of the dual-phase spiral CT scans classified this as a benign lesion. **(c)** T1-weighted (170/4.4; flip angle, 80°) Mn-DPDP–enhanced MR image shows marked, slightly inhomogeneous enhancement. The conspicuity of the lesion (white arrow) greatly improved because of the presence of an unenhanced hypointense rim (tumor capsule) marking the border of the lesion. Readers of the Mn-DPDP–enhanced MR images classified this lesion as HCC, which was histopathologically confirmed.

DPDP–enhanced MR imaging performs favorably compared with contrast-enhanced dual-phase spiral CT. These favorable results for Mn-DPDP–enhanced MR imaging were found for differentiating benign from malignant lesions and for characterizing lesions as either hepatocellular or nonhepatocellular. The comparison of ROC curves indicates that the classification of a lesion as either benign or malignant would be correct more often with Mn-DPDP–enhanced MR imaging than with dual-phase spiral CT (24). Also, radiologists were more confident of their interpretation of Mn-DPDP–enhanced MR images than of dual-phase spiral CT scans.

We should, however, discuss some benefits and limitations of the study before turning to the clinical consequences of our findings. First, the use of the same state-of-the-art equipment in all six centers for dual-phase spiral CT and for Mn-DPDP–enhanced MR imaging ensured that data could be pooled and compared. Comparison between modalities was also aided by the interpretation of lesions by the independent radiologists experienced in these techniques. Although not all images were read in duplo, when classifications of images differed between interpreters, a double reading and, when necessary, a consensus interpretation were performed. Overall results of the comparison between dual-phase spiral CT and Mn-DPDP–enhanced MR imaging after these further readings were not different from those of the first readings, and this resulted in a strengthening of the validity of the findings. We reported results of the first readings, as this situation best reflects clinical routine.

Second, the reference standard we used was based on all available imaging data combined with all available clinical data. Ethical considerations necessitated that we refrained from obtaining histopathologic data (which involves performing an invasive diagnostic procedure that carries a certain risk to the patient) when, on the basis of all available information, a lesion was considered benign or could already be diagnosed with great certainty. Although the lack of histopathologic confirmation could have led to misdiagnosis, we consider this undifferential because we found that discrepancies in diagnosis between Mn-DPDP–enhanced MR imaging and dual-phase spiral CT occurred as often in patients in whom diagnoses were histopathologically confirmed as they occurred in those in whom this confirmation was lacking. If anything, this misclassification would therefore have led to an underestimation of the differences between both imaging modalities. Additionally, including only patients with histopathologically proved diagnoses yielded the same results as including all patients for classifying the nature (malignant vs benign) and type of liver

lesions (hepatocellular vs nonhepatocellular).

Third, the latest Mn-DPDP–enhanced MR images were obtained approximately 1 hour after contrast material administration, and the latest dual-phase spiral CT images were obtained approximately 8 minutes after contrast material administration. Although obtaining 24-hour postcontrast Mn-DPDP–enhanced MR images would probably help to improve the characterization of certain liver lesions, as in some subtypes of HCC and colorectal liver metastasis, excretion of Mn-DPDP is impaired and the retention of Mn-DPDP persists, giving a characteristic late enhancement on Mn-DPDP–enhanced MR images. Also, the central scar of focal nodular hyperplasia and the pseudocapsule of HCC would become more conspicuous on 24-hour postcontrast Mn-DPDP–enhanced MR images than on 1-hour postcontrast images (25). On the other hand, obtaining postcontrast dual-phase spiral CT images at a later time would not have aided in the characterization of focal liver lesions. This is because the CT contrast agent has such a low affinity for liver tissue and is cleared so swiftly from the system that there would be no difference with 8-minute postcontrast images.

Although of no influence on the results, enhancement patterns of focal liver lesions on both Mn-DPDP–enhanced MR images and dual-phase spiral CT scans were not specifically recorded per patient. Therefore, the correlation between the enhancement pattern and the grade of HCC tumor differentiation could not be addressed. Previous studies have indicated that in patients with HCC the degree of Mn-DPDP uptake was closely related to the grade of tumor differentiation (11,15). This enhancement pattern can vary from generally homogeneous enhancement in well-differentiated HCC to irregular patchy or nodular enhancement or even entirely heterogeneous appearances in poorly differentiated lesions. Similar findings were also observed in contrast-enhanced CT studies of HCC (17,18,20).

Dual-phase spiral CT was associated with incorrect diagnoses concerning the type and the nature of focal liver lesions in a much wider disease spectrum than was Mn-DPDP–enhanced MR imaging. This variability in lesion characterization reflects that the appearance of liver lesions on dual-phase spiral CT scans is influenced by many physiologic, pathologic, and technical factors, besides lesion attributes (eg, neovascularity, grade of differentiation). This might have led to the erroneous classification of a lesion as shown in Figure 2 that was classified as benign, despite the fact that it lacked benign features, and to the classification of the lesion in Figure 3 that was interpreted as a calcification. At dual-phase spiral CT, atypical enhancement patterns of focal liver lesions are not uncommon, which complicates lesion characterization. In our study, this was reflected by the readers being less confident in characterizing a lesion as benign or malignant with dual-phase spiral CT than they were with Mn-DPDP–enhanced MR imaging, even when both classifications were correct.

Atypical Mn-DPDP–enhanced MR patterns are less common, and in our study, they mainly occurred in cases erroneously classified as HCC instead of as metastasis (Fig 4). However, because the rim-like enhancement on Mn-DPDP–enhanced MR images, as often seen in HCC, is theoretically unlikely to appear in metastases of the colon, we believe that some mistake might have been

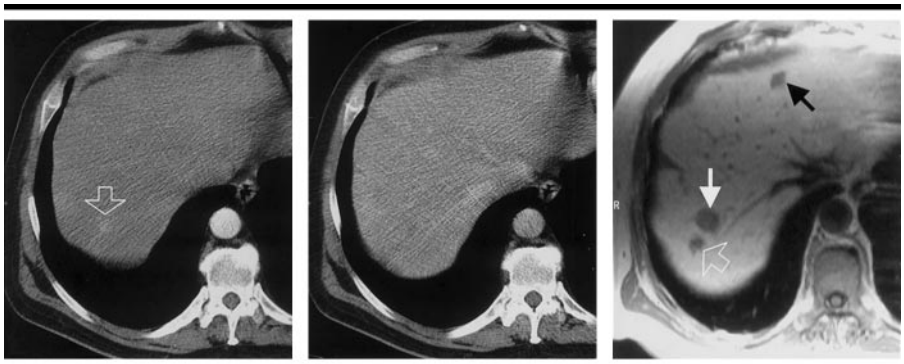

a. b. c.

Figure 3. Transverse images show liver metastases in a 56-year-old man. The suboptimal dual-phase spiral CT scans obtained in the **(a)** hepatic arterial phase and **(b)** portal venous phase show no focal lesions apart from a slightly hyperattenuating area (arrow in **a**) in the upper right hepatic lobe visible in **a** that was not classified as metastasis but as possible calcification. **(c)** On the T1-weighted (170/4.4; flip angle, 80°) Mn-DPDP–enhanced MR image, lesions can be seen with better contrast and conspicuity as hypointense lesions visible in the upper right hepatic lobe. Both posterior lesions were classified as metastasis (open and solid white arrows), and the anterior lesion (black arrow) was classified as benign. The histopathologic diagnosis of the posterior lesions was liver metastasis from adenocarcinoma of an unknown primary tumor.

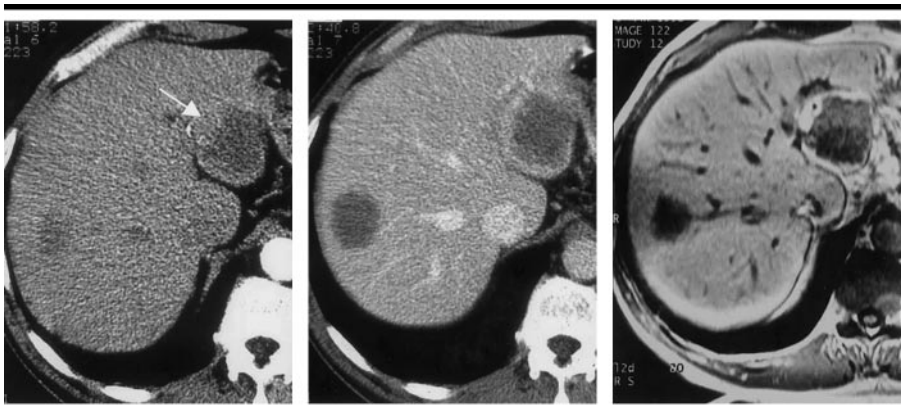

a. b. c.

Figure 4. Transverse images show multiple focal liver lesions in a 61-year-old man. Only the lesion located in the left hepatic lobe (arrow) was selected for evaluation. **(a)** Dual-phase spiral CT revealed a nonenhanced low-attenuating lesion on the image obtained in the arterial phase. **(b)** Scan obtained in the portal venous phase depicts faint peripheral zone enhancement. On the basis of findings of dual-phase spiral CT, metastasis was the diagnosis. **(c)** On the T1-weighted (170/4.4; flip angle, 80°) Mn-DPDP–enhanced MR image, the lesion demonstrates marked enhancement in the peripheral zone. Such rim-like enhancement was generally irregular in thickness and at some parts was nodular in shape. The central bulk of the lesion showed no obvious enhancement. On the basis of findings of Mn-DPDP–enhanced MR, the diagnosis was a malignant lesion of hepatocellular origin, possibly HCC. The histopathologic diagnosis was liver metastasis from primary colon carcinoma.

TABLE 2
Correctly Classified Diagnoses in 145 Patients and in 77 Patients with Histologically Confirmed Diagnoses

Correct Diagnoses	No. of Patients with Correct Diagnoses at Dual-Phase Spiral CT	No. of Patients with Correct Diagnoses at Mn-DPDP–enhanced MR Imaging	*P* Value
Overall	83 (57)	108 (74)	.001
	43 (56)*	57 (74)*	.004*
Differentiation between			
Malignant vs benign	98 (68)	123 (85)	.001
	53 (69)*	67 (87)*	.001*
Hepatocellular vs	93 (64)	130 (90)	.001
nonhepatocellular	57 (74)*	67 (87)*	.033*

Note.—Number in parentheses is the percentage.
* Data in 77 patients with histopathologically confirmed diagnoses.

TABLE 3
Sensitivity and Specificity in 145 Patients and in 77 Patients with Histologically Confirmed Diagnoses

Differentiation of Lesions and Data	Dual-Phase Spiral CT*	Mn-DPDP–enhanced MR Imaging*	*P* Value
Malignant vs benign			
Sensitivity			
	71 (69/97)	90 (87/97)	<.001†
	72 (47/65)†	91 (59/65)†	.002
Specificity			
	60 (29/48)	75 (36/48)	.17
	50 (6/12)†	67 (8/12)†	.63†
Hepatocellular vs nonhepatocellular			
Sensitivity			
	56 (20/36)	89 (32/36)	.008
	61 (14/23)†	91 (21/23)†	.07†
Specificity			
	67 (73/109)	90 (98/109)	<.001
	80 (43/54)†	85 (46/54)†	.50†

* Data are percentages. Data in parentheses are the number of diagnoses correctly identified by using the modality/total number correct.
† Data in 77 patients with histopathologically confirmed diagnoses.

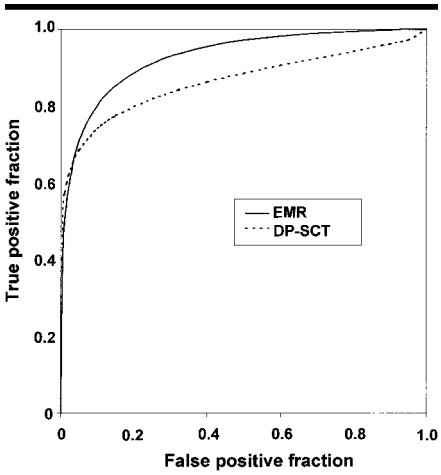

Figure 5. ROC comparative analysis of Mn-DPDP–enhanced MR imaging *(EMR)* and dual-phase spiral CT *(DP-SCT)* regarding the presence of a malignant lesion indicates better performance of Mn-DPDP–enhanced MR imaging compared with that of dual-phase spiral CT (difference between Mn-DPDP–enhanced MR and dual-phase spiral CT in the under-curve area = 0.07; $P = .03$).

made regarding the sampling or histopathologic diagnosis. The underlying mechanism for the occurrence of rim-like enhancement in some metastatic liver tumors has been attributed to several causes (26). First, peritumoral malignant infiltration into neighboring normal liver parenchyma can result in intermingling of nonhepatocellular malignant cells with normal functioning hepatocytes in the peripheral region of liver metastasis. Second, compression of surrounding normal liver tissue by a metastatic tumor mass may lead to impaired Mn-DPDP excretion or persistent Mn-DPDP retention because of the compressed bile canaliculi in these areas (26).

Kane et al (23) also reported such a rim-like enhancement phenomenon in a patient with cholangiocarcinoma, which is known to infiltrate neighboring normal liver tissue. Thus, although Murakami et al (11) stated that the peripheral enhancement phenomenon of metastases is unlikely to cause diagnostic confusion with HCC, we found this rim enhancement of some metastatic lesions so intense that a clear differentiation from poorly differentiated HCC, which is known to take up Mn-DPDP to a much lesser degree than typically well-differentiated HCC (15,22), could not be determined.

Despite our findings that Mn-DPDP–enhanced MR imaging is superior to dual-phase spiral CT for characterizing focal liver lesions, there are problems in implementing this outcome in patient care. Because of shortages in the times that MR imaging examinations can be scheduled (MR imaging is more time consuming and fewer machines are available) and cost issues, dual-phase spiral CT might remain the first-choice imaging modality for the majority of patients suspected of having pathologic focal liver lesions. In this case, Mn-DPDP–enhanced MR imaging could be reserved as a second-stage diagnostic tool (before turning to invasive procedures) when the diagnosis would still be inconclusive by using dual-phase spiral CT or other imaging findings combined with clinical information. Perhaps increasing the MR imager availability together with lowering prices for MR contrast agents may boost the role of MR imaging in examination of the liver. Since the time of this study, other liver-specific MR contrast agents (reticuloendothelial or hepatobiliary), such as gadoxetic acid disodium (Eovist; Schering, Berlin, Germany) and gadobenate dimeglumine (Multihance; Bracco, Milan, Italy), have been proposed and have potential for characterizing liver lesions (27–29).

Although promising, for now these agents have not been approved by the Food and Drug Administration, and since no findings of comparative studies of these agents have been published, their role is not yet certain. Also, new dynamic gadolinium-enhanced MR techniques for the classification of focal liver lesions show promising results. Because the performance of Mn-DPDP–enhanced MR imaging has not yet been compared with that of the newly developed dynamic gadolinium-enhanced MR imaging, it is not clear which technique is preferred, although both seem to surpass the performance of dual-phase spiral CT (30).

In conclusion, results from this multicenter study show that Mn-DPDP–en-

hanced MR imaging is safe and well tolerated and that it is superior to contrast-enhanced dual-phase spiral CT for distinguishing malignant from benign and hepatocellular from nonhepatocellular focal liver lesions.

Acknowledgment: We acknowledge Mary Roddie, MD, Charing Cross Hospital, London, England, for her help with the recruitment of patients into the study.

References

1. Rummeny EJ, Marchal G. Liver imaging: clinical applications and future perspectives. Acta Radiol 1997; 38:626–630.
2. Taylor HM, Ros PR. Hepatic imaging: an overview. Radiol Clin North Am 1998; 36:237–245.
3. Wittenberg J, Stark DD, Forman BH, et al. Differentiation of hepatic metastases from hepatic hemangioma and cysts by using MR imaging. AJR Am J Roentgenol 1988; 151:79–84.
4. Rummeny EJ, Wernecke K, Saini S, et al. Comparison between high-field-strength MR imaging and CT for screening of hepatic metastases: a receiver operating characteristic analysis. Radiology 1992; 182:879–886.
5. Whitney WS, Herfkens RJ, Jeffrey RB, et al. Dynamic breath-hold multiplanar spoiled gradient-recalled MR imaging with gadolinium enhancement for differentiating hepatic hemangiomas from malignancies at 1.5 T. Radiology 1993; 189:863–870.
6. Semelka RC, Shoenut JP, Ascher SM, et al. Solitary hepatic metastasis: comparison of dynamic contrast-enhanced CT and MR imaging with fat-suppressed T2-weighted, breath-hold T1-weighted FLASH, and dynamic gadolinium-enhanced FLASH sequences. J Magn Reson Imaging 1994; 4:319–323.
7. Yamashita Y, Mitsuzaki K, Yi T, et al. Small hepatocellular carcinoma in patients with chronic liver damage: prospective comparison of detection with dynamic MR imaging and helical CT of the whole liver. Radiology 1996; 200:79–84.
8. Ros PR, Freeny PC, Harms SE, et al. Hepatic MR imaging with ferumoxides: a multicenter clinical trial of the safety and efficacy in the detection of focal hepatic lesions. Radiology 1995; 196:481–488.
9. Seneterre E, Taourel P, Bouvier Y, et al. Detection of hepatic metastases: ferumoxides-enhanced MR imaging versus unenhanced MR imaging and CT during arterial portography. Radiology 1996; 200:785–792.
10. Oudkerk M, van den Heuvel AG, Wielopolski PA, Schmitz PIM, Borel Rinkes IHM, Wiggers T. Hepatic lesions: detection with ferumoxide-enhanced T1-weighted MR imaging. Radiology 1997; 203:449–456.
11. Murakami T, Baron RL, Peterson MS, et al. Hepatocellular carcinoma: MR imaging with mangafodipir trisodium (MnDPDP). Radiology 1996; 200:69–77.
12. Torres CG, Lundby B, Tufte Sterud A, McGill S, Gordon PB, Strand Bjerknes H. MnDPDP for MR imaging of the liver: results from the European phase III studies. Acta Radiol 1997; 38:631–637.
13. Rummeny EJ, Torres CG, Kurdziel JC, Nilsen G, Op de Beeck B, Lundby B. MnDPDP for MR imaging of the liver: results of an independent image evaluation of the European phase III studies. Acta Radiol 1997; 38:638–642.
14. Padovani B, Lecesne R, Raffaelli C, et al. Tolerability and utility of mangafodipir trisodium (MnDPDP) at the dose of 5 mumol/kg body weight in detecting focal liver tumors: results of a phase III trial using an infusion technique. Eur J Radiol 1996; 23:205–211.
15. Ni YC, Marchal G, Zhang XW, et al. The uptake of manganese dipyridoxal-diphosphate by chemically induced hepatocellular carcinoma in rats. Invest Radiol 1993; 28:520–528.
16. Hamm B, Vogl TJ, Branding G, et al. Focal liver lesions: MR imaging with MnDPDP—initial clinical results in 40 patients. Radiology 1992; 182:167–174.
17. Hollett MD, Jeffrey RB Jr, Nino-Murcia M, Jorgensen MJ, Harris DP. Dual-phase helical CT of the liver: value of arterial phase scans in the detection of small (< or = 1.5 cm) malignant hepatic neoplasms. AJR Am J Roentgenol 1995; 164: 879–884.
18. van Leeuwen MS, Noordzij J, Feldberg MAM, Hennipman AH, Doornewaard H. Focal liver lesions: characterization with triphasic spiral CT. Radiology 1996; 201: 327–336.
19. Baron RL, Oliver JH III, Dodd GD III, Nalesnik M, Holbert BL, Carr B. Hepatocellular carcinoma: evaluation with biphasic, contrast-enhanced, helical CT. Radiology 1996; 199:505–511.
20. van Hoe L, Baert AL, Gryspeerdt S, et al. Dual-phase helical CT of the liver: value of an early-phase acquisition in the differential diagnosis of noncystic focal lesions. AJR Am J Roentgenol 1997; 168: 1185–1192.
21. Oliver JH III, Baron RL. Helical biphasic contrast-enhanced CT of the liver: technique, indications, interpretation, and pitfalls. Radiology 1996; 201:1–14.
22. Rofsky NM, Weinreb JC, Bernardino ME, Young SW, Lee JK, Noz ME. Hepatocellular tumors: characterization with MnDPDP-enhanced MR imaging. Radiology 1993; 188:53–59.
23. Kane PA, Ayton V, Walters HL, et al. MnDPDP-enhanced MR imaging of the liver: correlation with surgical findings. Acta Radiol 1997; 38:650–654.
24. Hanley JA, NcNeill BJ. The meaning and use of the area under a receiver operating characteristic (ROC) curve. Radiology 1982; 143:29–36.
25. Coffin CM, Diche T, Mahfouz AE, et al. Benign and malignant hepatocellular tumors: evaluation of tumoral enhancement after mangafodipir trisodium injection on MR imaging. Eur Radiol 1999; 9:444–449.
26. Ni YC, Marchal G, Yu J, et al. Experimental liver cancers: MnDPDP-enhanced rims in MR-microangiographic-histologic correlation study. Radiology 1993; 188:45–51.
27. Hahn PF, Saini S. Liver-specific MR imaging contrast agents. Radiol Clin North Am 1998; 36:287–297.
28. Mahfouz AE, Hamm B, Taupitz M. Contrast agents for MR imaging of the liver: a clinical review. Eur Radiol 1997; 7:507–513.
29. Imam K, Bluemke DA. MR imaging in the evaluation of hepatic metastases. Magn Reson Imaging Clin North Am 2000; 8:741–756.
30. Semelka RC, Martin DR, Balci C, Lance T. Focal liver lesions: comparison of dual-phase CT and multisequence multiplanar MR imaging including dynamic gadolinium enhancement. J Magn Reson Imaging 2001; 13:397–401.